Clin Orthop Relat Res (2009) 467:2149–2158
DOI 10.1007/s11999-009-0776-z

ORIGINAL ARTICLE

Tibia Adaptation after Fibula Harvesting

An in Vivo Quantitative Study

Fulvia Taddei PhD, Matteo Balestri MS, Eugenio Rimondi MD, Marco Viceconti PhD, Marco Manfrini MD

Received: 18 June 2008 / Accepted: 23 February 2009 / Published online: 10 March 2009

Abstract Absence of the fibula after harvesting to reconstruct an upper-limb segment increases loads on the donor-side tibia and thereby provides a unique opportunity to analyze the bone adaptation process in humans. We therefore quantified densitometric and morphologic changes of the donor-side tibia in three young patients (ages 8, 13, 16 years), on the basis of computed tomography (CT) examinations of both legs (one preoperatively and two postoperatively). The range of final followup was 27–43 months. Three-dimensional models of shank bones were generated from CT data and used to measure cross-sectional area, diaphyseal cortical thickness, and cross-sectional moment of inertia. In addition, density of the newly formed bone was evaluated. The donor-side tibia showed morphologic and density adaptation with time. New bone was deposited predominantly in the interosseous space and almost replaced the bone area lost by excision of the fibula. The second moment of area grew more in the donor-side tibia than in the intact one, without fully recovering the contralateral tibia-fibula complex values, and the principal axes rotated toward the preoperative direction. Thus, while considerable adaptation had occurred by 27–43 months in these young patients, the adaptation was incomplete; the mineral density of the newly formed bone recovered normal cortical bone values only in the patient with the longest followup (43 months). **Level of Evidence:** Level IV, therapeutic study. See the Guidelines for Authors for a complete description of levels of evidence.

One or more of the authors (MM) have received funding from the AIRC (Associazione Italana per la Ricerca sul Cancro) Foundation. Each author certifies that his or her institution has approved or waived approval for the human protocol for this investigation, that all investigations were conducted in conformity with ethical principles of research, and that informed consent for participation in the study was obtained.

F. Taddei (✉), M. Balestri, M. Viceconti
Laboratorio di Tecnologia Medica, Istituto Ortopedico Rizzoli, Via di Barbiano, 1/10, 40136 Bologna, Italy
e-mail: taddei@tecno.ior.it

E. Rimondi
Radiology Department, Istituto Ortopedico Rizzoli, Bologna, Italy

M. Manfrini
Oncology Department, Istituto Ortopedico Rizzoli, Bologna, Italy

Introduction

The vascularized fibula graft (VFG) is an important approach for treating long-bone defects or difficult nonunions. Transplantation of the ipsilateral fibula, although not vascularized, was first used successfully by Huntington in 1905 to fill a 12.7-cm tibial defect in a 7-year-old boy [17], but only in the mid1970s [35] was free transfer of a VFG using microvascular techniques described. Its use has increased [42] and today is used in demanding skeletal reconstructive treatments (eg, segmental bony defects [19], osteomyelitis [43], kyphosis [27], or congenital tibial pseudarthrosis [39]). It is used particularly to reconstruct massive bone defects (greater than 10 cm) after tumor excision [4, 9, 11, 16]. Donor-site morbidity has been reported as a consequence of VFG harvesting [3, 10, 25, 32, 36] but generally is considered acceptable when weighed against the potential benefits [8, 36]. However, nontraumatic fractures of the donor-side tibia are still reported although as single sporadic cases [7, 18, 20, 29, 40, 41]. These fractures could be explained in principle by excessive tibial loading

resulting from fibula removal before complete tibia adaptation, as the fibula reportedly has a weightbearing function (1% to 30% of the total load) [13, 22, 34, 38]. However, the process and timing of tibial adaptation to changes in the biomechanical environment in humans is not completely understood.

Despite the fact that several studies qualitatively described evolution of the donor-side leg after VFG [1, 3, 10, 25, 32, 36], these did not quantitatively describe adaptation of the donor-side tibia. Questionnaire results [1, 3, 30, 36], disability scales [1, 10, 25], or gait analyses [3, 25] have been reported in some studies, and disabilities such as pain, ankle instability, and inability to run have been described [1, 3, 10, 18, 25, 30, 32, 36]. Other studies have attempted quantitative analyses of long-term side effects based on radiographs [2, 10, 14, 28, 30]. Most of these studies, however, focused on ankle deformities [2, 10, 28, 30], and only one described thickening of the tibial lateral cortex [14]. In contrast, experimental studies performed on animals have reported quantitative analyses of radius adaptation after ulna resection for pigs [15] and sheep [23, 26]. Histomorphometric measurements, second moment of inertia calculations [23], and bone density adaptation [26] were reported. All studies consistently concluded the donor-side radius adapted within 12 to 50 weeks after ulna harvesting. Strain measurements performed either in vitro [26] or in vivo [23] showed strain levels recovered values similar to or smaller than those recorded in the intact condition. These animal studies suggest the donor-side tibia can fully adapt and recover the mechanical strength of the original complex, but results of the studies cannot be applied directly for humans. When VFG is used to reconstruct an upper-limb segment, the primary alteration induced in the lower limbs is increased load on the donor-side tibia. This provides a unique opportunity to analyze the bone adaptation process to altered biomechanical conditions in humans.

Our aim therefore was to quantify donor-side tibia adaptation after VFG harvesting to confirm whether the adaptation seen in animals is true in humans. We specifically compared in the tibia on the donor side with its contralateral control, the (1) cross-sectional area (CSA), (2) cortical thickness, (3) cross-sectional moment of inertia (CSMI) and principal axes orientations, and (4) mineral density of the new-formed bone.

Materials and Methods

We identified three patients who underwent VFG for intercalary humerus reconstruction from among the six available patients who underwent surgery during the previous 4 years when the study began and who had complete CT examinations. These patients provided informed consent and were enrolled in the study. No patient was affected by any musculoskeletal disorder or deformity of the lower limbs. For all patients, a major intercalary portion of the fibula, contralateral to the reconstructed humerus, was harvested and no screw was used to stabilize the ankles. The patients were two boys (Patients A and B) and one girl (Patient C) aged 8, 13, and 16 years, respectively, at the time of surgery; the diagnoses were Ewing's sarcoma (Patients A and C) and osteosarcoma (Patient B) (Table 1). Measures were taken preoperatively and at two followups in these three patients: the minimum first followup was 9 months (mean, 12 months; range, 9–14 months) and the minimum second followup was 27 months (mean, 33 months; range, 27–43 months).

Table 1. Patient demographics and resection information

Demographic	Patient		
	A	B	C
Gender	Male	Male	Female
Age (years)	8	13	16
Side	Right	Right	Left
Resection region*	B–D	B–D	B–E
Fibula length (mm)	268	355	339
Resection length (mm)	135	140	184
First followup (months)	9	14	13
Second followup (months)	27	43	29

* Resection regions are shown in Fig. 2.

Each patient had preoperative CT (CT1) at the shank level and two equivalent CT examinations (CT2 and CT3) during followup approximately 1 and 2 years after surgery, respectively (Fig. 1); CT examinations were performed with a General Electric High Speed Advantage CT scanner (General Electric Corp, Fairfield, CT) (Table 2). Patients wore a cast on the donor-side leg for 3 weeks after surgery, and load-bearing was allowed incrementally during the next 2 weeks. After this period, all patients were allowed full load-bearing.

Three transverse sections at the level of the harvested fibula were identified for each patient and replicated in all three CT data sets. Measurements of morphologic features of bone and density were performed on these corresponding sections. We first created three-dimensional (3-D) models of the shank bone segments for both limbs from each CT data set using semiautomatic segmentation software (Amira® v 4.1; Mercury Computer Systems, Inc, Chelmsford, MA) (Fig. 2).

To create a shank reference axis, we identified four anatomic landmarks on each 3-D model through virtual palpation [33] using DataManager© [37] software: tibial tuberosity (TT), head of fibula (HF), lateral malleolus

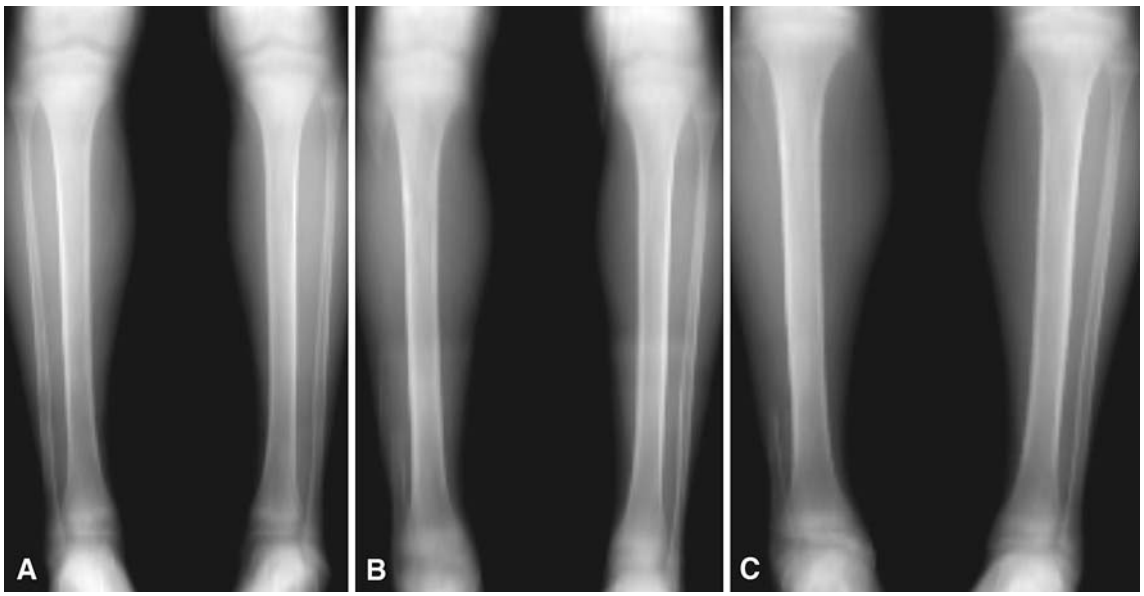

Fig. 1A–C Digitally reconstructed plain radiographs obtained from the CT data sets for Patient A taken (**A**) preoperatively and at (**B**) first and (**C**) second followups are shown.

Table 2. Details of the CT examinations

Patient	CT examination	KVP (kV)	XR current (mA)	Pixel size (mm)	Diaphysis		Epiphysis	
					Slice thickness (mm)	Slice spacing (mm)	Slice thickness (mm)	Slice spacing (mm)
A	Preoperative	120	240	0.467	3	2	3	2
	First followup	120	200	0.547	5	5	5	5
	Second followup	120	180	0.547	5	4	3	2
B	Preoperative	120	200	0.527	5	4	3	2
	First followup	120	200	0.547	5	5	5	5
	Second followup	120	200	0.703	5	4	3	2
C	Preoperative	120	200	0.664	5	4	3	2
	First followup	120	200	0.586	5	4	3	2
	Second followup	120	200	0.586	3	2	3	2

CT = computed tomography; KVP = peak kilovoltage; XR = xray.

(LM), and medial malleolus (MM). The reference axes were created using the identified landmarks according to the method described by Cappozzo et al. [5]: the origin was located at the midpoint between the malleoli (MM and LM); the vertical axis (y) was defined by the intersection of the quasifrontal plane (LM, MM, HF) and quasisagittal plane (midpoint between the malleoli, TT and orthogonal to quasifrontal plane). The z axis lay in the quasifrontal plane and the x axis was orthogonal to the yz plane (Fig. 2).

On the preoperative CT scans, we divided the fibula length (distance from the head of the fibula to lateral malleolus) into six segments, and three midpoints (proximal, intermediate, distal) were identified in each bone model (Fig. 2). The corresponding sections in each CT data set were identified for both limbs. In all but one patient (most distal section of Patient B), these sections corresponded to the portion of the harvested fibula. This procedure allowed identification of the corresponding sections in the tibia, taking into consideration patient growth during followup.

We measured bone CSAs on the three sections using the UGS CAD software (v 5.0; Siemens Product Lifecycle Management Software, Inc, Plano, TX).

The CSA of the tibia (tibiaCSA), fibula (fibulaCSA), and total bone (totalCSA = tibiaCSA + fibulaCSA) were calculated for each section for both limbs. The difference between the tibiaCSA at the followups and the tibiaCSA

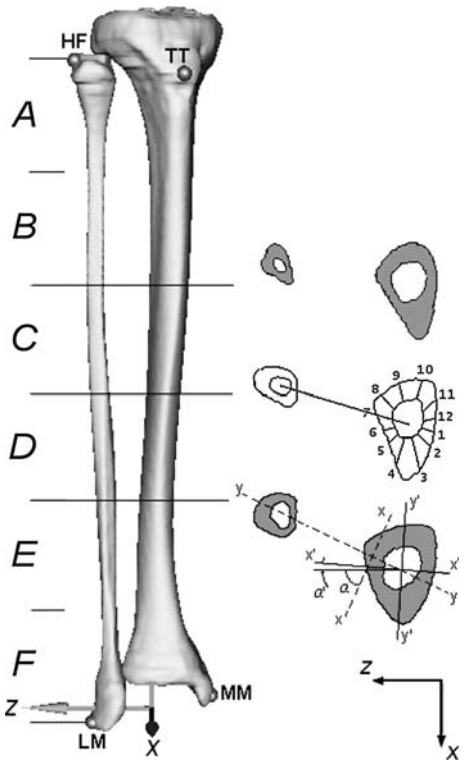

Fig. 2 On the left is the 3-D model of the tibia and fibula for Patient B. The four landmarks (TT, HF, LM, MM) and the anatomic reference system are visible. On the right, the three sections are identified to perform measurements. In the intermediate section, the 12 angular sectors (30° wide) used for the cortical thickness evaluation are shown. In the distal section, the diagram illustrates the principal axes of inertia of the tibia-fibula complex (xx, yy) and the corresponding direction of the tibia alone (x′x′, y′y′). TT = tibial tuberosity; HF = head of fibula; LM = lateral malleolus; MM = medial malleolus.

during the preoperative examination was calculated, averaged over the three sections, and reported as a percentage of the preoperative value. To distinguish adaptive bone remodeling from physiologic bone growth, the ratio between the donor-side tibiaCSA and the contralateral side was computed and averaged over the three sections.

To measure the tibial cortical thickness in a reproducible way, all cross sections were divided into 12 angular sectors (30° wide) starting from the direction of the segment that joins the tibia and fibula centroids (Fig. 2). In the event of a missing fibula, the direction of the first segment was recovered, using, as a reference, the anatomic reference system of the segment and reproducing the angle between the x axis and the segment joining the two centroids calculated in the preoperative model. Finally, measurement of cortical thickness was calculated for each angular sector, averaged for the three sections, and reported as a percentage.

To assess the ability of the bone to resist bending, we calculated, for each 3-D model, the maximum and minimum CSMI of the tibia-fibula complex (I_{xx}, I_{yy}) and the tibia alone ($I_{x'x'}$, $I_{y'y'}$) (Fig. 2) on the three sections using UGS CAD software and then averaged. We also performed an analysis of orientation of the principal axes. The angle between the principal axis of the cross-sectional geometry and the mediolateral anatomic axis (z) was measured. The angle between the z-axis and the principal axis (xx) of the tibia-fibula complex was named α; the angle between the z-axis and the principal axis of the tibia alone (x′x′) was named α'. Rotation of the principal axis of the tibia alone (x′x′) during followup was measured and compared with the same measurement performed in the contralateral tibia.

All CT data sets were calibrated with the European Spine Phantom [21] to derive mineral density values from Hounsfield units (HU). The profile of HU for the tibia of the donor-side leg along the direction joining the tibia and fibula centroids, Direction 7, was analyzed using OSIRIS software (v 4.19; University Hospital of Geneva, Geneva, Switzerland). To distinguish newly formed from existing bone, we assumed all new bone lay on the periosteal side. This assumption is supported partially by published results for animals [23] and by preliminary measurements performed on the CSA of the endosteal canal that in no case showed a reduction. Each measurement was repeated three times and average values are reported.

The differences in mineral density values among the newly formed bone, preexisting tibial cortical bone in the donor side, and cortical bone in the contralateral tibia were determined by an analysis of variance test performed on the distributions of the measured density values (Scheffe post hoc test).

In Patient B, the morphologic measurements were repeated on nine equally spaced cross sections to test if the results could be influenced by the number of midpoints considered. A nonparametric Kolmogorov-Smirnov test was performed to ascertain nonsignificant differences ($p > 0.05$ in all cases). Because of the substantial effort needed to perform and analyze all measurements, only the three midpoints were considered in the other two patients. The results therefore were relative to measurements obtained for the three corresponding cross sections in all patients.

Results

All parameters showed the donor-side tibia remodeled after VFG. The effect of fibula osteotomy was consistent in all three patients: the tibiaCSA of the donor-side leg grew substantially more than that of the contralateral leg (Fig. 3 A). Only In Patient B did the contralateral tibia show a cross section reduction at the first followup. At the last followup, the donor-side tibiaCSA was on average 32% greater than the contralateral side for all patients. The measurements of total bone area showed the total CSAs of both limbs were

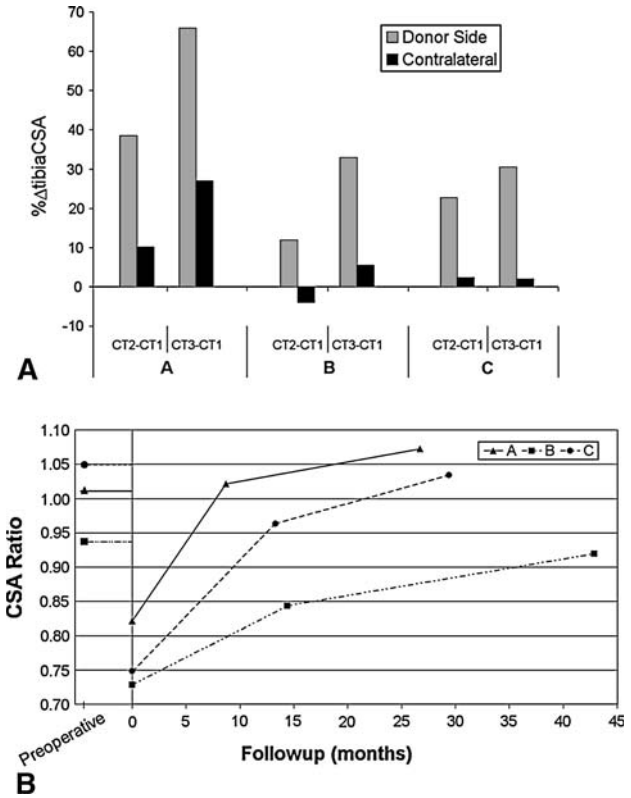

Fig. 3A–B (**A**) A graph shows the changes in percent tibiaCSA between followups (CT2, CT3) and preoperative examination (CT1) in Patients A, B, and C. The changes are given in percentage form with respect to preoperative values. (**B**) This graph shows the ratio between donor side tibiaCSA and contralateral totalCSA during followup for Patients A, B, and C. The ratio between totalCSA of the surgically treated and contralateral limbs before fibula excision is reported on the negative abscissa axis. CSA = cross-sectional area.

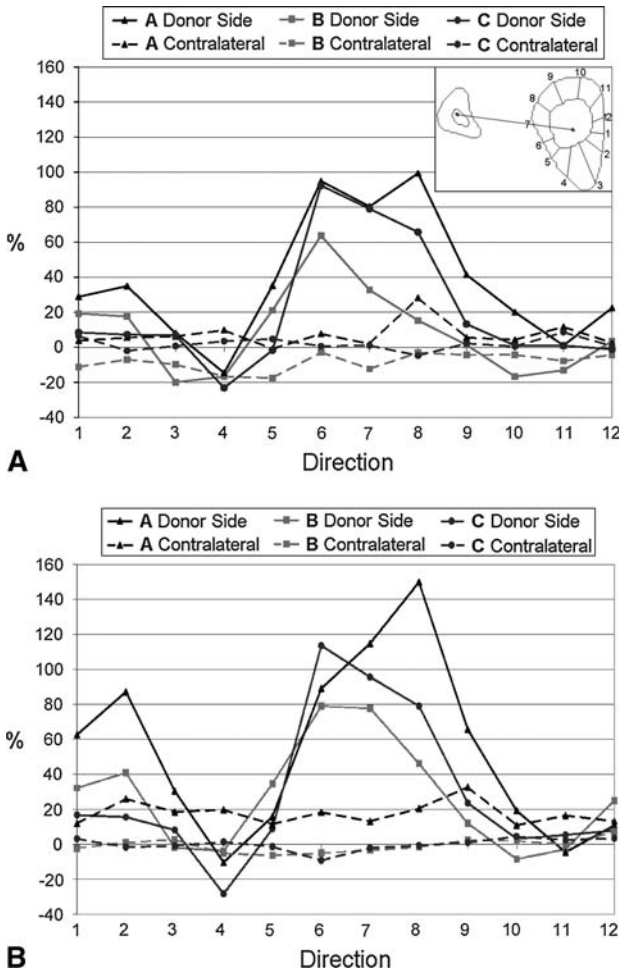

Fig. 4A–B The graphs show the increase with respect to the preoperative value of the tibia cortical thickness at the (**A**) first and (**B**) second followups. A schematic of the 12 directions considered is superimposed on the top right of (**A**).

essentially equal at the time of surgery, and at the last followup, the newly formed bone in the donor-side tibia was almost equal to the area of the harvested fibula (Fig. 3B). In Patient A, the youngest patient, the tibiaCSA exceeded the contralateral totalCSA at the last followup. In addition, it was calculated the fibulaCSA represented 21% ± 2% of totalCSA in all preoperative CT data sets.

For all patients, measurements of cortical thickness in radial directions showed the newly formed bone in the donor-side tibia was deposited predominantly at the level of the interosseous space (Directions 6 and 8) (Figs. 4, 5). This pattern, already present at the first followup, became more evident by last followup. More limited but evident growth was recorded in the diametrically opposite direction (Directions 12, 1–2). A loss of cortical bone was registered in the anterior direction (Direction 4). The increase of the cortical bone thickness of the contralateral tibia was almost uniform in all directions.

For all patients, the maximum and minimum CSMI of the donor-side tibia increased more than those of the contralateral tibia during followup (Table 3). The maximum moment at the last followup was on average 27% greater than that in the contralateral tibia, whereas the minimum moment was on average 65% greater than the corresponding contralateral one. In no case, however, did the CSMI of the donor-side tibia reach values comparable to the CSMI of the contralateral tibia-fibula complex. Even after 3 years, the principal moments of inertia were not re-equilibrated between the two legs. The adapted tibia managed to recover, on average, the minimum CSMI (81% of the contralateral complex) but could not compensate on the other direction because the maximum CSMI reached, on average, only 22% of the contralateral value. Immediately after fibula harvesting, the angle between the principal axis and the mediolateral direction changed 90°, 72°, and 75° for Patients A, B, and C, respectively. During followup, as a result of the tibia adaptation, the principal axis of inertia rotated toward the preoperative direction

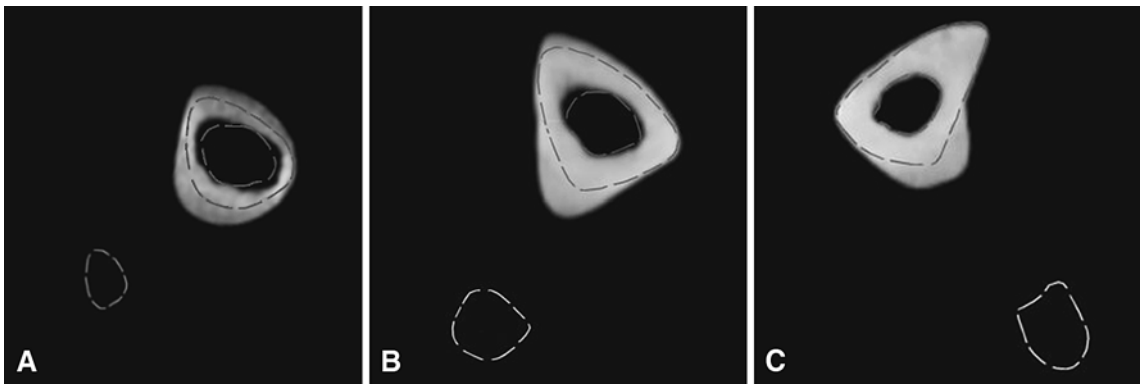

Fig. 5A–C The medial sections of the donor-side tibia at the last followup of (**A**) Patient A, (**B**) Patient B, and (**C**) Patient C are shown. The dashed lines are the tibia and fibula profiles in the corresponding sections before surgery. The asymmetry of the newly deposited bone is evident.

Table 3. The CSMI (mm^4) of the tibia and the tibia-fibula complex, when present, for all patients during followup

	Patient A			Patient B			Patient C		
	Preoperative	9 months	27 months	Preoperative	14 months	43 months	Preoperative	13 months	29 months
I_{xx}									
Donor total	22,349			84,084			92,446		
Donor tibia	4218	6026	9101	13,851	15,155	19,417	11,835	14,023	15,081
Contralateral total	23,040	26,944	32,322	90,080	93,085	107,695	69,835	73,149	72,594
Contralateral tibia	4187	4854	6312	14,732	15,063	16,859	11,829	12,260	12,540
I_{yy}									
Donor total	4327			13,657			11,803		
Donor tibia	2678	4581	6166	7430	10,220	12,985	4393	7633	8711
Contralateral total	4303	5037	6546	14,636	14,799	16,566	11,464	11,998	12,172
Contralateral tibia	2540	2996	3783	8427	8537	9450	4374	4419	4451

CSMI = cross-sectional moment of inertia; I_{xx}, I_{yy} = maximum and minimum cross-sectional moment of inertia.

(Fig. 6). In none of the three patients was the original direction fully recovered; the differences between the original I_{xx} axis and the $I_{x'x'}$ axis at the last followup were 44°, 34°, and 60° for Patients A, B, and C, respectively. The direction of the principal axis in the contralateral tibia-fibula complex and in the tibia alone did not adapt during this time (Fig. 6).

The density of the newly formed bone was less than the average cortical density in the same bone and in the intact contralateral bone, but it increased between the first and second followups (Fig. 7). At the second followup, the percentage differences between mean density values of newly formed bone and contralateral bone were 10%, 3%, and 7% for Patients A, B, and C, respectively. At both followups for Patient A, the cortical bone of the donor-side tibia showed a lower density than the contralateral tibia. The newly formed bone density at the last followup was still less than the density of the contralateral tibia cortical bone for all patients.

Discussion

The process and timing of adaptation of bones in humans is not well understood quantitatively. Absence of the fibula after harvesting for reconstruction elsewhere increases loads on the donor-side tibia and thereby provides a unique opportunity to study bone adaptation in humans. Therefore, we quantitatively evaluated the adaptation process of the tibia in humans having an absent fibula. We specifically compared the (1) CSA, (2) cortical thickness, (3) CSMI and principal axes orientations, and (4) mineral density of the new-formed bone of the donor-side tibia with those of the contralateral tibia.

The major limitation of our study is the limited number of patients. Only three patients of differing ages were considered. We believe this does not invalidate the conclusions given the consistent behavior among all subjects. The majority of patients undergoing VFG were not eligible for this study because the harvested fibula was used to

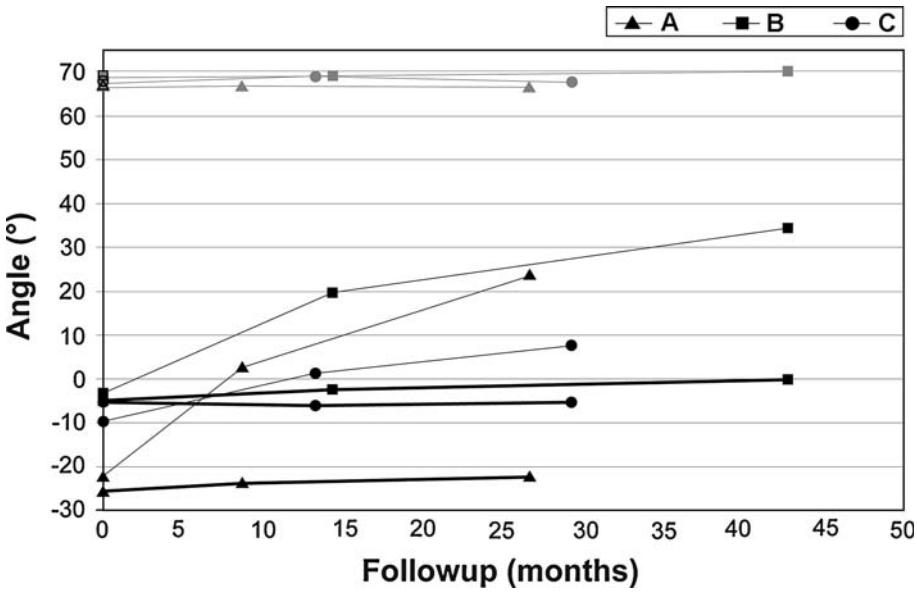

Fig. 6 A graph shows, for each patient, the principal axis angle evolution for the cross-sectional geometry of the tibia-fibula complex (α-angle) and for the tibia alone (α′-angle) toward the mediolateral anatomic axis (*z*). The thin gray lines represent the evolution of the contralateral α-angle; the thick black lines represent the evolution of the contralateral α′-angle. The thin black lines represent the evolution of the donor-side α′-angle. The empty black marks on the y-axis represent the values of α before fibula excision.

reconstruct a lower limb bone. In those cases, the simultaneous presence of two major alterations of the skeletal structure would prevent isolation of the VFG harvesting effects. It is possible even reconstruction of an upper limb segment might introduce asymmetries in gait patterns that could influence the adaptive response of the tibia. However, this appears an unavoidable but still minor effect that can be ignored. Another limitation concerns the impossibility to assess whether the adaptive remodeling process was completed at the last followup. With only two postoperative examinations, we could not assess whether a stable condition was reached. A final limitation is all patients underwent chemotherapy as a result of their disease and this may have influenced the time needed for the adaptation process. However, even if the absolute adaptive remodeling rate were influenced [12], chemotherapy affects both limbs equally; therefore, the comparison between the adaptation of the donor-side tibia and the contralateral tibia is valid.

The adaptation in terms of amount and location of new bone formation was consistent for all patients. After VFG the donor-side tibia adapted in terms of morphologic features and density. Approximately 2 years after surgery, the CSA of the donor-side tibia was almost equal to the total CSA of the contralateral tibia-fibula complex. The location of new bone deposition was asymmetric and predominantly directed toward the missing fibula. This altered cross-sectional morphology reflected a change of the tibia CSMI and orientation of principal axes. The second moment of area grew more in the donor-side tibia than in the contralateral tibia and the principal axes rotated toward the direction of the preoperative axes. Newly formed bone in all patients had a mineral density increase through followup, but only for Patient B with the longest followup did the density reach a value comparable to the contralateral cortical one (97%). This suggests that in Patient B, the process of recovering normal cortical bone density was almost completed, whereas further adaptation can be expected for the other two patients given the shorter followup times. In Patient A, the youngest, the adaptive response was more rapid and evident. This may be related to young age and to a chemotherapy protocol that did not require postoperative treatment. In Patient B, a reduction of the tibia CSA of the intact leg was recorded at the first followup. This behavior, different from that of the other two patients, may be the result of the specific chemotherapy protocol used to treat osteosarcoma.

In the only study analyzing the morphologic adaptation of the donor-side tibia in humans [14], thickening on the lateral aspect was observed. This is consistent with our results because the newly formed bone in the interosseous space would appear predominantly on the lateral aspect of the tibia when imaged with planar radiography. Our results are consistent with those seen in animal studies [15, 23, 26] where radius adaptation completely compensated the CSA lost by removal of the ulna and occurred mostly toward the former interosseous space. Similar to our findings, two studies [15, 23] showed the newly formed bone was deposited predominantly at the periosteal aspect of the radius. This is partially in contrast with the substantial endosteal bone apposition described by Lee and Taylor [26]. The only density evaluation was performed by Lee and Taylor [26], who reported the newly formed bone recovered values typical of mature cortical bone in 24 weeks. We found a similar trend, although a direct comparison of the mineralization rate cannot be performed owing to the different bone metabolism among species. Our data suggest 3½ years may be required before the mineralization process is complete.

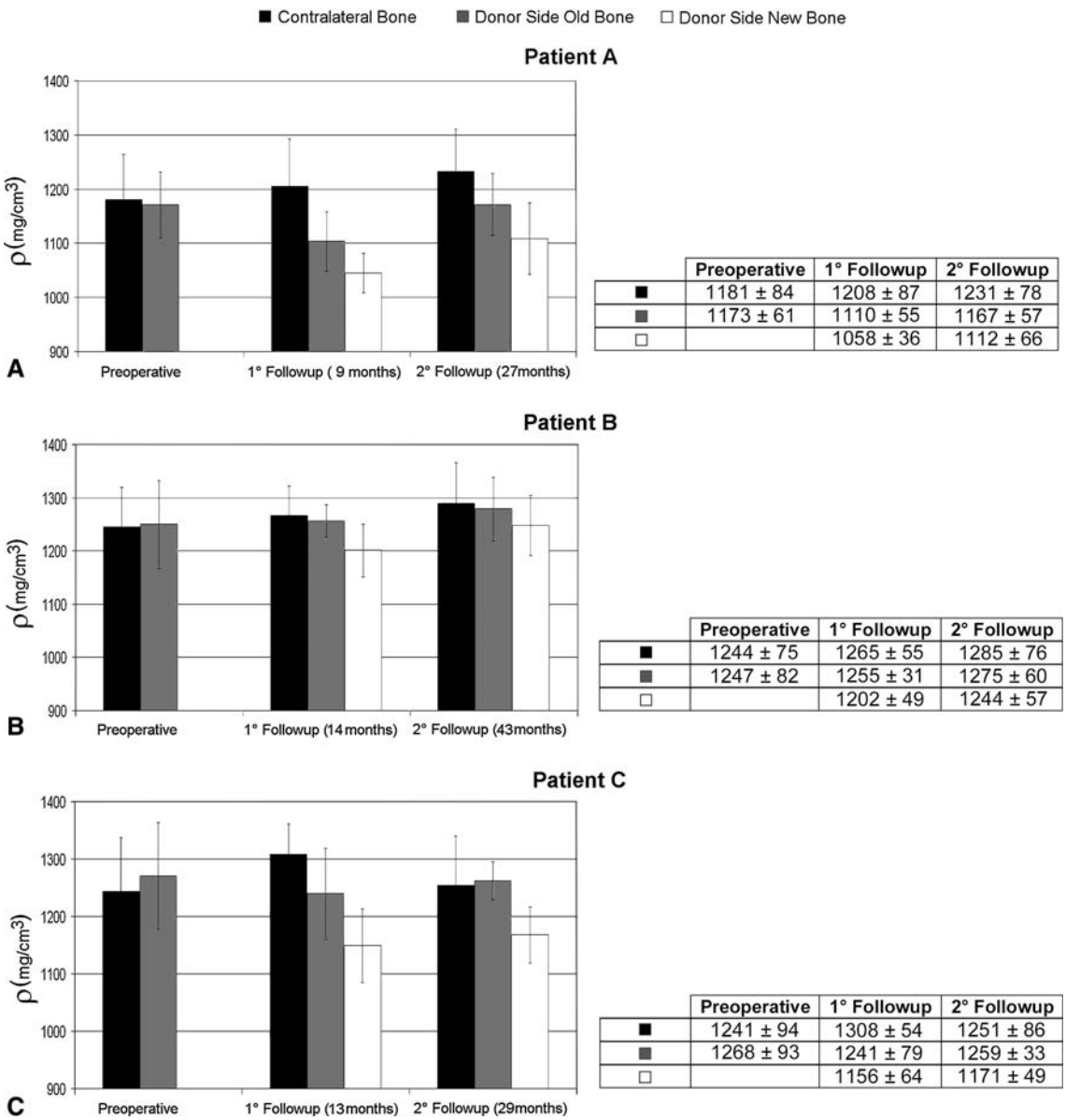

	Preoperative	1° Followup	2° Followup
■	1181 ± 84	1208 ± 87	1231 ± 78
■	1173 ± 61	1110 ± 55	1167 ± 57
□		1058 ± 36	1112 ± 66

	Preoperative	1° Followup	2° Followup
■	1244 ± 75	1265 ± 55	1285 ± 76
■	1247 ± 82	1255 ± 31	1275 ± 60
□		1202 ± 49	1244 ± 57

	Preoperative	1° Followup	2° Followup
■	1241 ± 94	1308 ± 54	1251 ± 86
■	1268 ± 93	1241 ± 79	1259 ± 33
□		1156 ± 64	1171 ± 49

Fig. 7A–C The graphs show the density (ρ) of newly formed bone, preexisting bone, and cortical bone of the contralateral tibia for (**A**) Patient A, (**B**) Patient B, and (**C**) Patient C during followup. Error bars = standard deviations. The exact values of mean and standard deviations are shown in the relative tables.

The fibula has a weightbearing function and therefore, removal of a VFG increases tibia load levels. The donor-side tibia reacted with a positive adaptation to the absence of the ipsilateral fibula, suggesting it could be able to recover the weightbearing competency of the normal tibia-fibula complex, at least in growing patients. To confirm this and therefore derive direct indications for the rehabilitation program, we must know the magnitude and distribution of loads acting on the tibia-fibula complex during motion, but these still are unclear. A few in vitro studies [13, 22, 34, 38] suggest under physiologic loads, the tibia and fibula are loaded principally in compression with the fibula bearing between 1% to 30% of the total load, which is consistent with the fibulaCSA/totalCSA ratio we measured. However, these studies could not account for muscle forces. Several studies attempted to measure in vivo deformation of the tibia during motion [6, 24, 31], but data were obtained for a limited number of points and not for the tibia and fibula together.

Our data corroborate the hypothesis that the tibia can recover the mechanical features of the original complex. The CSA of the donor-side tibia compensated the area lost after fibula harvesting in all patients. Therefore, the ability to sustain axial loads, which seem predominant, would be fully

recovered once the density recovery process was completed. This is consistent with the fact that all spontaneous fractures reported in the donor-side tibia [7, 18, 20, 29, 40, 41] were in mature patients (31–82 years of age) and at a short time after surgery (1–16 months), when the adaptive remodeling of the tibia likely was deficient or incomplete. Care should be taken in concluding that axial load is the predominant loading condition because newly formed bone showed marked asymmetry, suggesting the contemporary presence of a bending load. This may be the result of the eccentricity of the knee reaction with respect to the resisting tibia cross section as a consequence of the fibula harvesting. However, it also could be the result of a bending moment generated by the muscles' action. More likely, the real condition is a combination of the two, but the measurements we performed cannot make these distinctions.

Our data show harvesting a substantial segment of the fibular diaphysis induces, in growing patients, an adaptive bone remodeling of the tibia that seems to compensate for the induced biomechanical impairment. Our results confirm prior observations in animal studies, and establish a time frame during which bone adaptation can occur.

Acknowledgments We thank Dr Massimo Ceruso who performed the vascular microsurgery in all patients, Luigi Lena for the illustrations, and Mauro Ansaloni for support during the data analysis.

References

1. Anthony JP, Rawnsley JD, Benhaim P, Ritter EF, Sadowsky SH, Singer MI. Donor leg morbidity and function after fibula free flap mandible reconstruction. *Plast Reconstr Surg.* 1995;96:146–152.
2. Babhulkar SS, Pande KC, Babhulkar S. Ankle instability after fibular resection. *J Bone Joint Surg Br.* 1995;77:258–261.
3. Bodde EW, de Visser E, Duysens JE, Hartman EH. Donor-site morbidity after free vascularized autogenous fibular transfer: subjective and quantitative analyses. *Plast Reconstr Surg.* 2003;111:2237–2242.
4. Capanna R, Campanacci DA, Belot N, Beltrami G, Manfrini M, Innocenti M, Ceruso M. A new reconstructive technique for intercalary defects of long bones: the association of massive allograft with vascularized fibular autograft. Long-term results and comparison with alternative techniques. *Orthop Clin North Am.* 2007;38:51–60, vi.
5. Cappozzo A, Catani F, Croce UD, Leardini A. Position and orientation in space of bones during movement: anatomical frame definition and determination. *Clin Biomech (Bristol, Avon).* 1995; 10:171–178.
6. Ekenman I, Halvorsen K, Westblad P, Fellander-Tsai L, Rolf C. Local bone deformation at two predominant sites for stress fractures of the tibia: an in vivo study. *Foot Ankle Int.* 1998;19: 479–484.
7. Emery SE, Heller JG, Petersilge CA, Bolesta MJ, Whitesides TE Jr. Tibial stress fracture after a graft has been obtained from the fibula: a report of five cases. *J Bone Joint Surg Am.* 1996;78:1248–1251.
8. Farhadi J, Valderrabano V, Kunz C, Kern R, Hinterman B, Pierer G. Free fibula donor-site morbidity: clinical and biomechanical analysis. *Ann Plast Surg.* 2007;58:405–410.
9. Fuchs B, Ossendorf C, Leerapun T, Sim FH. Intercalary segmental reconstruction after bone tumor resection. *Eur J Surg Oncol.* 2008;34:1271–1276.
10. Ganel A, Yaffe B. Ankle instability of the donor site following removal of vascularized fibula bone graft. *Ann Plast Surg.* 1990;24:7–9.
11. Ghert M, Colterjohn N, Manfrini M. The use of free vascularized fibular grafts in skeletal reconstruction for bone tumors in children. *J Am Acad Orthop Surg.* 2007;15:577–587.
12. Glasser DB, Duane K, Lane JM, Healey JH, Caparros-Sison B. The effect of chemotherapy on growth in the skeletally immature individual. *Clin Orthop Relat Res.* 1991;262:93–100.
13. Goh JC, Mech AM, Lee EH, Ang EJ, Bayon P, Pho RW. Biomechanical study on the load-bearing characteristics of the fibula and the effects of fibular resection. *Clin Orthop Relat Res.* 1992;279:223–228.
14. Gonzalez-Herranz P, del Rio A, Burgos J, Lopez-Mondejar JA, Rapariz JM. Valgus deformity after fibular resection in children. *J Pediatr Orthop.* 2003;23:55–59.
15. Goodship AE, Lanyon LE, McFie H. Functional adaptation of bone to increased stress: an experimental study. *J Bone Joint Surg Am.* 1979;61:539–546.
16. Hsu RW, Wood MB, Sim FH, Chao EY. Free vascularised fibular grafting for reconstruction after tumour resection. *J Bone Joint Surg Br.* 1997;79:36–42.
17. Huntington TW. VI. Case of bone transference: use of a segment of fibula to supply a defect in the tibia. *Ann Surg.* 1905;41: 249–251.
18. Ivey M, Hicks CA, Hook JD. Stress fracture of the tibia after harvest of a vascularized fibular graft for repair of nonunion of the humerus. *Orthopedics.* 1995;18:57–60.
19. Jupiter JB, Bour CJ, May JW Jr. The reconstruction of defects in the femoral shaft with vascularized transfers of fibular bone. *J Bone Joint Surg Am.* 1987;69:365–374.
20. Kabadaya MS, Beausang E, Stassen LF. Stress fracture of the tibia following a vascularised free fibular flap. *J Plast Reconstr Aesthet Surg.* 2008;61:e21–23.
21. Kalender WA, Felsenberg D, Genant HK, Fischer M, Dequeker J, Reeve J. The European Spine Phantom: a tool for standardization and quality control in spinal bone mineral measurements by DXA and QCT. *Eur J Radiol.* 1995;20:83–92.
22. Lambert KL. The weight-bearing function of the fibula: a strain gauge study. *J Bone Joint Surg Am.* 1971;53:507–513.
23. Lanyon LE, Goodship AE, Pye CJ, MacFie JH. Mechanically adaptive bone remodelling. *J Biomech.* 1982;15:141–154.
24. Lanyon LE, Hampson WG, Goodship AE, Shah JS. Bone deformation recorded in vivo from strain gauges attached to the human tibial shaft. *Acta Orthop Scand.* 1975;46:256–268.
25. Lee EH, Goh JC, Helm R, Pho RW. Donor site morbidity following resection of the fibula. *J Bone Joint Surg Br.* 1990;72:129–131.
26. Lee TC, Taylor D. Quantification of ovine bone adaptation to altered load: morphometry, density, and surface strain. *Eur J Morphol.* 2003;41:117–125.
27. Minami A, Kasashima T, Iwasaki N, Kato H, Kaneda K. Vascularised fibular grafts: an experience of 102 patients. *J Bone Joint Surg Br.* 2000;82:1022–1025.
28. Nathan SS, Hung-Yi L, Disa JJ, Athanasian E, Boland P, Cordeiro PG, Healey JH. Ankle instability after vascularized fibular harvest for tumor reconstruction. *Ann Surg Oncol.* 2005;12:57–64.
29. Pacifico MD, Floyd D, Wood SH. Tibial stress fracture as a complication of free-fibula vascularised graft for mandibular reconstruction. *Br J Plast Surg.* 2003;56:832–834.
30. Papadopulos NA, Schaff J, Bucher H, Groener R, Geishauser M, Biemer E. Donor site morbidity after harvest of free

osteofasciocutaneous fibular flaps with an extended skin island. *Ann Plast Surg.* 2002;49:138–144.
31. Rolf C, Westblad P, Ekenman I, Lundberg A, Murphy N, Lamontagne M, Halvorsen K. An experimental in vivo method for analysis of local deformation on tibia, with simultaneous measures of ground reaction forces, lower extremity muscle activity and joint motion. *Scand J Med Sci Sports.* 1997;7:144–151.
32. Shpitzer T, Neligan P, Boyd B, Gullane P, Gur E, Freeman J. Leg morbidity and function following fibular free flap harvest. *Ann Plast Surg.* 1997;38:460–464.
33. Taddei F, Ansaloni M, Testi D, Viceconti M. Virtual palpation of skeletal landmarks with multimodal display interfaces. *Med Inform Internet Med.* 2007;32:191–198.
34. Takebe K, Nakagawa A, Minami H, Kanazawa H, Hirohata K. Role of the fibula in weight-bearing. *Clin Orthop Relat Res.* 1984;184:289–292.
35. Taylor GI, Miller GD, Ham FJ. The free vascularized bone graft: a clinical extension of microvascular techniques. *Plast Reconstr Surg.* 1975;55:533–544.
36. Vail TP, Urbaniak JR. Donor-site morbidity with use of vascularized autogenous fibular grafts. *J Bone Joint Surg Am.* 1996;78:204–211.
37. Viceconti M, Taddei F, Montanari L, Testi D, Leardini A, Clapworthy G, Van Sint Jan S. Multimod Data Manager: a tool for data fusion. *Comput Methods Programs Biomed.* 2007;87:148–159.
38. Wang Q, Whittle M, Cunningham J, Kenwright J. Fibula and its ligaments in load transmission and ankle joint stability. *Clin Orthop Relat Res.* 1996;330:261–270.
39. Weiland AJ, Weiss AP, Moore JR, Tolo VT. Vascularized fibular grafts in the treatment of congenital pseudarthrosis of the tibia. *J Bone Joint Surg Am.* 1990;72:654–662.
40. Westesson PL, Wandtke JC. Stress fracture of the tibia: an unusual complication of reconstructive surgery of the mandible. *J Oral Maxillofac Surg.* 1999;57:70–74.
41. Wolf BR, Buckwalter JA. Tibial stress fracture following fibular graft harvesting: a case report. *Iowa Orthop J.* 2001;21:68–72.
42. Wood MB. Free vascularized fibular grafting-25 years' experience: tips, techniques, and pearls. *Orthop Clin North Am.* 2007;38:1–12, v.
43. Zalavras CG, Femino D, Triche R, Zionts L, Stevanovic M. Reconstruction of large skeletal defects due to osteomyelitis with the vascularized fibular graft in children. *J Bone Joint Surg Am.* 2007;89:2233–2240.